


Article

Catalytic Co-Pyrolysis of *Mesua ferrea* L. De-Oiled Cake and Garlic Husk in the Presence of Red-Mud-Based Catalysts

Abhishek Kumar, Janaki Komandur, Vasu Chaudhary and Kaustubha Mohanty * 

Department of Chemical Engineering, Indian Institute of Technology Guwahati, Guwahati 781039, India; abhishekk.cl@iitg.ac.in (A.K.); kjanaki@iitg.ac.in (J.K.); vasuchaudhary001@gmail.com (V.C.)

* Correspondence: kmohanty@iitg.ac.in

Abstract: Utilizing lignocellulosic biomass as a renewable energy source for the production of sustainable fuel is of paramount importance. This study focuses on the catalytic co-pyrolysis of *Mesua ferrea* L. de-oiled cake (MDC) and Garlic husk (GH) as potential feedstocks for bio-fuel production. The pyrolysis experiments were conducted using a semi-batch reactor under inert conditions at temperatures of 500, 550, and 600 °C, with a heating rate of 10 °C min⁻¹, a particle size below 1 mm, and an inert gas flow rate of 80 mL min⁻¹. The findings reveal that temperature significantly influences the yield of pyrolytic products. However, GC-MS analysis detected higher oxygenated compounds in the bio-oil, negatively impacting its heating value. To improve fuel quality, co-pyrolysis with and without a catalyst for a feedstock ratio of 1:1 w/w was performed. Red mud, an alkaline waste mainly composed of Fe₂O₃, Al₂O₃, and SiO₂, is a hazardous environmental concern from aluminum production and is used as a catalyst. The red-mud catalysts reduced oxygen concentration and increased carbon content, acidity, and heating value in the pyrolytic oil. GC-MS analysis of the bio-oil confirmed that using catalysts combined with MDC and GH significantly decreased the concentration of acidic and aromatic compounds, thereby improving the pyrolytic oil's higher heating value (HHV).

Keywords: *Mesua ferrea* L. de-oiled cake; garlic husk; catalytic co-pyrolysis; red-mud; Ni/RM



Citation: Kumar, A.; Komandur, J.; Chaudhary, V.; Mohanty, K. Catalytic Co-Pyrolysis of *Mesua ferrea* L. De-Oiled Cake and Garlic Husk in the Presence of Red-Mud-Based Catalysts. *Catalysts* **2023**, *13*, 1401. <https://doi.org/10.3390/catal13111401>

Academic Editors: Gartzzen Lopez and Maite Artetxe

Received: 12 August 2023

Revised: 12 October 2023

Accepted: 24 October 2023

Published: 28 October 2023



Copyright: © 2023 by the authors. Licensee MDPI, Basel, Switzerland. This article is an open access article distributed under the terms and conditions of the Creative Commons Attribution (CC BY) license (<https://creativecommons.org/licenses/by/4.0/>).

1. Introduction

The increase in demand for the world's energy consumption is bringing focus to the dependence on the renewable energy sector. Fossil fuels contribute to over 80% of the world's primary energy consumption. This leads to severe pollution of air, soil, and water [1]. Using biomass as a feedstock for producing renewable fuels and chemicals, particularly liquid fuels, shows tremendous energy security [2]. Pyrolysis is a method that can convert biomass into a liquid fuel known as bio-oil. This process has the potential to be both efficient and cost-effective. The different components of biomass, i.e., cellulose, hemicellulose, and lignin, decompose into various pyrolytic products, namely condensable gases (bio-oil), solid char, and non-condensable gases. Undesirable properties such as high acidity, low energy potential, and high-water content restrict the use of pyrolytic oil as a natural alternative to fossil fuel [3]. Co-pyrolysis is regarded as one of the most straightforward strategies for successfully and efficiently utilizing a wide variety of feedstocks while only requiring the amount of energy that is required for each individual feedstock. Co-pyrolysis has the potential to utilize a sizable amount of waste as a raw material, resulting in the efficient handling of waste. Furthermore, co-pyrolysis has the potential to drastically reduce energy consumption, cost of production, and processing times. The heating value and pyrolytic liquid production are increased by co-pyrolyzing the biomass feed [4].

Some of the raw materials used in the production of biofuels include non-edible oil seeds (vegetable oil), wheat husk, algal biomass, de-oiled cake, waste products, etc. The production of biofuels from agricultural waste, including non-edible oil crops, has

been the subject of much research and experimentation [5]. Pyrolysis and co-pyrolysis technologies can be used to produce value-added chemicals from these types of wastes and biodiesel revenue creation from non-edible oil seeds. The protein-rich cake was commonly used as fertilizer or as feed for livestock. Since too many de-oiled cakes are left over from the seed-pressing process to extract oil, they could be used to make energy and chemicals with added value [6]. *Mesua ferrea* L., often known as cobra saffron, grows abundantly in India's northeast. It is also accessible via Sri Lanka, southern Nepal, and Malaysia [5]. In this study, the de-oiled cake (MDC) produced from *Mesua ferrea* L. oilseed is being investigated as a potential feedstock for bioenergy. The direct application of most de-oiled cakes is hindered by the presence of undesirable anti-nutritive components and hazardous chemicals; this is especially true for cakes made from non-edible seeds. Therefore, it is essential to investigate further alternative applications for a significant quantity of de-oiled cakes. Not only does the process of converting de-oiled cakes into valuable commodities and biofuels help solve the problem of where to dispose of them, but it also provides an additional answer to the problems that exist in the energy sector [7]. Garlic husk (*Allium sativum*) is in the same family as onions that are used in cooking and medicine in many places worldwide, including Asia, North Africa, Central America, and the Middle East. The annual worldwide production of garlic (*Allium sativum*) is around 20-million tons. China and India are the major producers of garlic. From the years 2018–2019, India alone produces around 1.1-million tons of garlic, with Rajasthan and Uttar Pradesh as the two major garlic-producing states in India, followed by Gujrat, Punjab, and Assam. In India, the *Allium sativum* is the second-most cultivated bulb crop after onion. Around 30% of garlic constituents are solid waste, namely garlic husk and garlic straw. Hence, garlic waste produces significant amounts of solid agro-waste annually [8].

Studies on the co-pyrolysis of two or more different types of lignocellulosic feedstocks suggested that this is an efficient process to recover the organic chemicals [9]. Nevertheless, different raw materials mix and pyrolyze in a particular ratio, which still needs to be improved to produce high-quality fuel products. For example, when SS and poplar sawdust were co-pyrolyzed with a feedstock ratio of 1:0.15, the higher heating value (HHV) of the bio-oil was 27.5 MJ kg^{-1} , which is significantly less than the HHV ($40\text{--}45 \text{ MJ kg}^{-1}$) of existing fossil-based fuels. Pyrolytic bio-oil has several oxygen-containing molecules, producing highly viscous and acidic liquid, with poor HHV of the bio-oil [10]. Hence, it becomes crucial to incorporate an additional step to enhance the application of bio-oil further.

Catalytic pyrolysis accelerates the process, improving the quality and quantity of the products. A catalyst facilitates the breakdown of long-chain unsaturated fatty compounds to short-chain hydrocarbons. Combining biomass with the suitable catalysts improved conversion efficiency, decreased tar formation, and maximized product yield. Numerous studies are reported in the literature discussing the increase in the yield of pyrolytic liquid. Over the course of the past three decades, significant progress has been made in the field of catalytic pyrolysis, and this trend has only accelerated over the course of the past decade. For the purpose of pyrolysis, a great number of catalytic systems have been developed, such as noble and non-noble metal catalysts supported by zeolites, silica, and alumina [11]. However, because of their high cost, limited availability, low stability, and susceptibility to inactivation by water, attention has been placed on the design and development of cost-effective and easily accessible pyrolysis catalysts. Recently, catalysts made from wastes (red mud, charcoal, eggshell, etc.) have been considered. Therefore, waste can be utilized economically as raw material for pyrolysis [12].

The solid waste product produced during alumina manufacturing by Bayer's process is referred to as red mud. It is a mixture of metallic oxides such as Fe_2O_3 , CaO , SiO_2 , and NaOH . The presence of metallic compounds makes the waste even more complex and unsuitable for disposal [13]. Generally, red mud as a solid waste is utilized as a catalyst in many thermochemical conversion applications, including the pyrolysis of waste plastic and the hydrodeoxygenation of bio-oil. Only limited studies are available on using red mud in biomass pyrolysis. For instance, the co-pyrolysis of sewage sludge and rice husk

in various biochar catalysts was found to increase the production of hydrocarbons while lowering oxygenated and nitrogen-containing molecules [14].

In this study, we suggest an environmentally friendly and efficient technique for co-pyrolyzing *Mesua ferrea* L. de-oiled cake and garlic husks with a red-mud catalyst made from waste. The quality of the bio-oil that was produced was examined using gas chromatography-mass spectrometry (GC-MS) and FTIR analysis in order to compare the performances of thermal, co-pyrolysis, and catalytic co-pyrolysis. The hydrocarbon production pathway and catalytic mechanism were also detailed.

2. Results and Discussions

2.1. Physicochemical Characterization of Biomass Feedstock

The biomass feedstocks' physical and chemical properties were estimated using proximate/CHNS analysis. From the analysis reported in Table 1, it can be seen that the moisture content of the feed materials is less than 10%, indicating that the liquid pyrolysis product will contain less water content. Additionally, the volatile content of MDC and GH is significantly high, i.e., 81% and 66.8%, respectively. More vapor organic compounds (gases and liquids) are produced during the decomposition of biomass with a high volatile content than biomass with a relatively low volatile content [5]. During pyrolysis, biomass should also have less ash. A lower percentage of ash (4.86% for MDC and 11% for GH) contributes to a faster burning rate, simultaneously reducing the slag that forms at elevated pyrolysis temperatures [15]. This results in a significant increase in the pyrolysis of biomass and a reduction in the cost of operation. High ash concentration causes poor sample pyrolysis and waste disposal. The energy value of biomass is significantly influenced by its fixed carbon content. In order to get the most out of the pyrolysis process that generates heat, it is best to select biomass with a higher percentage of fixed carbon [16]. According to the findings, the biomass feedstocks chosen for this study have a low fixed carbon content (9.2 and 12.8% for MDC and GH, respectively) compared to another lignocellulosic biomass. Biomass contains carbon (C), hydrogen (H), oxygen (O), nitrogen (N), and sulfur (S). When compared to coal, biomass often has higher percentages of H and O and lower amounts of C, N, and S. Carbon and hydrogen are significant contributors to the heat that is produced during the combustion process. The amounts of these elements, as well as oxygen that were found in MDC and GH feedstocks (presented in Table 1), were comparable to the amounts that were discovered in other lignocellulosic wastes [16]. So, for energy purposes, fuels with a low oxygen concentration and a high carbon content are preferred. Since biomass contained just a trace quantity of sulphur and nitrogen, it was determined that the amount of pollution produced by the emission of non-condensable gases could decrease [17].

Table 1. A comparison of literature of physicochemical characterization of MDC and GH.

Properties	<i>Mesua ferrea</i> L. De-Oiled Cake (Present Study)	Groundnut De-Oiled Cake [6]	<i>Jatropha Curcas</i> De-Oiled Cake [18]	Garlic Husk (Present Study)	Rice Husk [19]	Coffee Husk [17]
Moisture content	4.08	5.6	0.44	6.8	8.43	9.06
Volatile content	82.63	83	79.2	71.5	68.25	77.09
Ash content	4.82	4.8	1.5	10.3	14.83	3.55
Fixed carbon	8.46	6.6	18.86	11.4	16.92	19.36
C	48.63	46.36	53.39	42.1	39.48	46.41
H	7.38	7.015	6.81	4.6	5.71	6.33
N	3.65	6.89	0.45	0.34	0.665	2.66
S	-	0.287	0.12	0.09	0.1	0.09
O	40.34	39.438	29.27	52.87	54.12	44.51
GHV (MJ kg ⁻¹)	18.86	15	19.11	14.01	17.34	18.5
Cellulose	56.91	-	16.47	41.32	41.52	47.29
Hemicellulose	29	-	50.31	29.34	14.04	15.57
Lignin	14.09	-	25.91	17.17	33.67	27.14

2.2. Functional Group Analysis of Biomass, Catalyst and Bio-Oil

The functional groups present in both the biomass and the catalyst were analysed using an FTIR spectroscopic technique. From the analysis, it was found that the C-H bond at 2875 cm^{-1} wave number is a symmetrical stretch present in the aliphatic alkene and alkyl groups present in the biomass [16]. A significant C-O stretch was also noticed at 1350 cm^{-1} , indicating a polar covalent bond that can be found in all the major components of the lignocellulosic biomass. The presence of the H-vibration in the phenyl rings can also be seen in garlic husk. This analysis essentially revealed the information related to the various functional groups and their bonding present within the various classification of compounds of MDC and GH, as seen in Figure 1a.

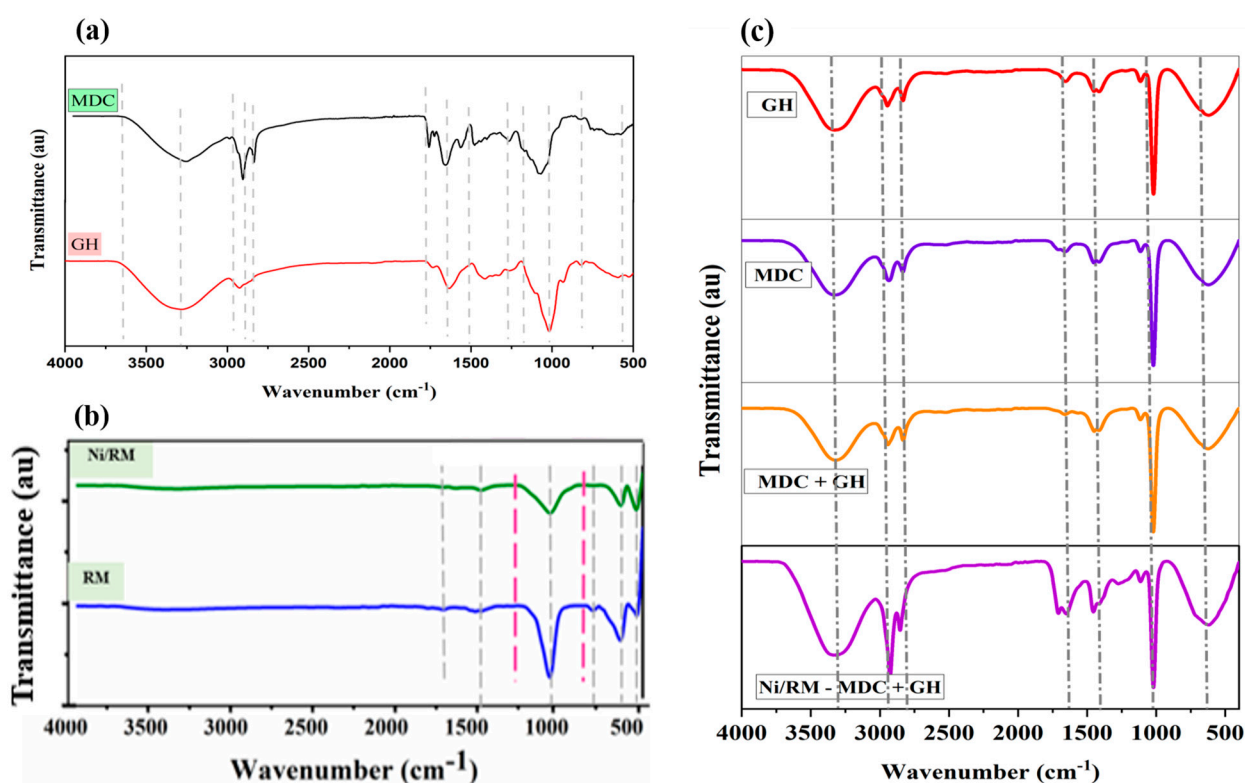


Figure 1. FTIR analysis of (a) biomass, (b) red-mud catalysts, and (c) bio-oil of different types of pyrolysis conditions.

The characteristics of the IR spectra of all the synthesized samples can be seen in Figure 1b. A stretching vibration of Si-O-Si in RM was observed at 1001 cm^{-1} . This stretching was also observed in all the catalysts, which may be due to the dissociation of this bond. A characteristic peak at 530 cm^{-1} was attributed to the stretching vibrations of Fe-O in RM. A relatively weak spectra of Al-O vibrations were detected in all the samples at 680 cm^{-1} and 750 cm^{-1} , which are related to $\gamma\text{-Al}_2\text{O}_3$. In addition, a weak spectrum was observed at 880 cm^{-1} , which is related to the Ca-O group. The characteristic vibrations at 1397 cm^{-1} of NiO can also be found in Figure 1b, indicating the impregnation of these metals on RM support material [20].

Figure 1c represents the FTIR analysis of bio-oil. The presence of hydroxyl-containing substances can be deduced from the presence of absorbance peaks at 3385 cm^{-1} . These peaks suggest the O-H vibrations. The appearance of absorbance peaks due to C-H bonds in the ranges of $2840\text{--}3000\text{ cm}^{-1}$ is indicative of the availability of alkanes and alkenes [16]. The 1715 cm^{-1} peak indicated carbonyl functional groups (C=O). Similar to this, peaks at 1674 cm^{-1} show that bio-oil contains C=C chemical bonds. The N-O bond was indicated by a $1500\text{--}1600\text{ cm}^{-1}$ peak. This spectrum demonstrates the presence of various kinds of organic molecules in bio-oil, including phenols, aliphatic alcohols, alkanes, alkenes, aro-

matics, ketones, and aldehydes, as well as compounds containing nitrogen and carboxylic acids and halides.

2.3. Thermal Decomposition of Biomass

Thermogravimetric analyser was used to evaluate the thermal and co-pyrolysis (1:1 *w/w*) degradation behaviour of *Mesua ferrea* L. de-oiled cake (MDC) and garlic husk (GH) at a heating rate of $10\text{ }^{\circ}\text{C min}^{-1}$. The TG-DTG behaviour of the different types of feedstocks can be seen in Figure 2. The thermal and co-pyrolysis degradation behaviour of biomass constituents (cellulose, hemicellulose, and lignin) can be divided into three distinct zones. The thermal and co-pyrolysis degradation of *Mesua ferrea* L. de-oiled cake (MDC) and garlic husk (GH) is initiated with the dehydration zone up to $150\text{ }^{\circ}\text{C}$, which involves the evaporation of moisture and light-volatile hydrocarbons [5]. The first significant mass loss typically occurs at around $70\text{--}75\text{ }^{\circ}\text{C}$ due to the evaporation of free moisture present in feedstock, whereas the small peak is at $150\text{ }^{\circ}\text{C}$, which may be attributed to the removal of bound moisture or the volatilization of very light components. The maximum breakdown is observed in the following active pyrolytic zone ($150\text{--}650\text{ }^{\circ}\text{C}$), where hemicellulose and cellulose are continuously heated to break them down into smaller molecules (hot volatiles). Up to $650\text{ }^{\circ}\text{C}$, there was active pyrolysis, which led to weight losses of 76.265%, 60.36%, and 66% for MDC, GH, and MDC + GH, respectively. At temperatures over $650\text{ }^{\circ}\text{C}$, biochar is eventually generated and is suitable for a variety of uses because the hydroxyl phenolic chemicals in lignin decrease the rate of thermal breakdown [16].

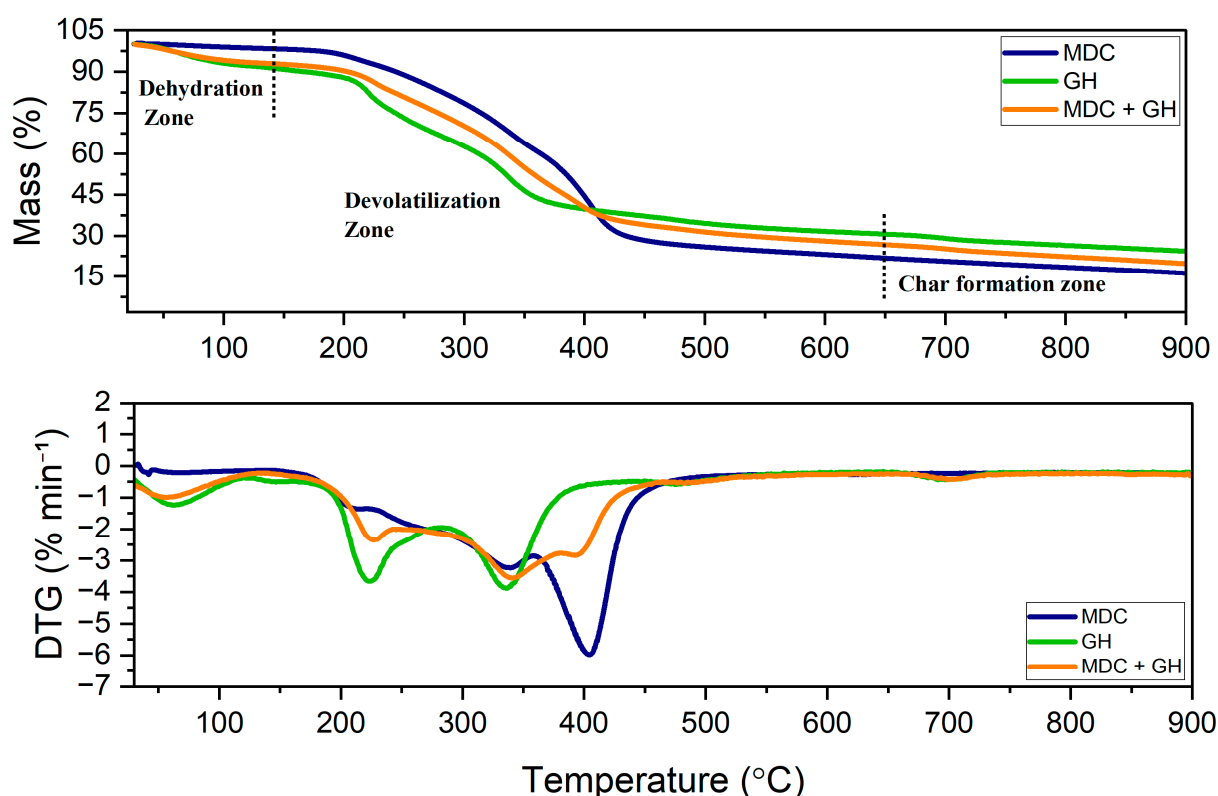


Figure 2. Thermal decomposition of behaviour of biomass and co-feed.

The early phases of the evaporation of water and light hydrocarbons were seen in the DTG profiles Figure of MDC, GH, and MDC + GH. In the instance of MDC, the first and second peaks at $216\text{ }^{\circ}\text{C}$ and $338\text{ }^{\circ}\text{C}$, respectively, proved hemicellulose breakdown, whereas the third peak at $406\text{ }^{\circ}\text{C}$ confirmed cellulose decomposition. The first and second peaks for GH at 194 and $225\text{ }^{\circ}\text{C}$ and the third peak at $337\text{ }^{\circ}\text{C}$, respectively, confirmed the breakdown of hemicelluloses and cellulose. Meanwhile, the first and second peaks for co-pyrolysis

at 224 °C and 347 °C, respectively, indicated the breakdown of hemicelluloses, while the third peak at 398 °C confirmed the decomposition of cellulose. Due to a slower breakdown and a lesser amount of lignin present in the biomass, the absence of any sharper peaks was noticed [21].

2.4. Characterization of Catalyst

2.4.1. Surface Area Analysis by BET

The surface area (SA) of all the calcined catalysts was found using BET analysis. The size and volumes of the pores of all the catalysts prepared were in the range of 11–25 nm and 0.1–0.16 cc g⁻¹. This indicates that the pores formed are mesoporous. The surface area analysis found that the specific SA of the freshly calcined red-mud support was 37.84 m² g⁻¹, which was higher than the mono metallic-impregnated catalyst [22]. In comparison to RM support, there was a prominent decrease in the SA of the metal-doped catalysts due to the blockage of the active surface sites by Ni metal [12]. The specific surface area of the Ni/RM was noted to be 24.91 m² g⁻¹. Additionally, the information about pore size revealed that the doping of Ni metal on RM support increased the pore size (22.42 nm) compared to RM support (11.12 nm).

2.4.2. Morphological Analysis of Catalysts by FESEM

Field emission scanning electron microscopy was employed to study the surface morphological nature of the catalyst. Figure 3a shows the random structures on RM support material, indicating agglomeration of the particles. Observations from FESEM images indicate that some minute particles adhere to larger particles. Therefore, the particle sizes are likely to be polydisperse, i.e., different sizes. From Figure 3b, Ni dispersion on the RM support indicates an agglomeration on the catalyst support with elongated particles. This agglomeration led to blocking active pores and reducing the surface area of the metal-impregnated catalyst. Further, a highly accumulated RM support is seen in Figure 3b due to the impregnation of the catalyst. In addition, the curvy shape of the particles indicates a mixture of micro and mesoporous nature of the catalyst [13].

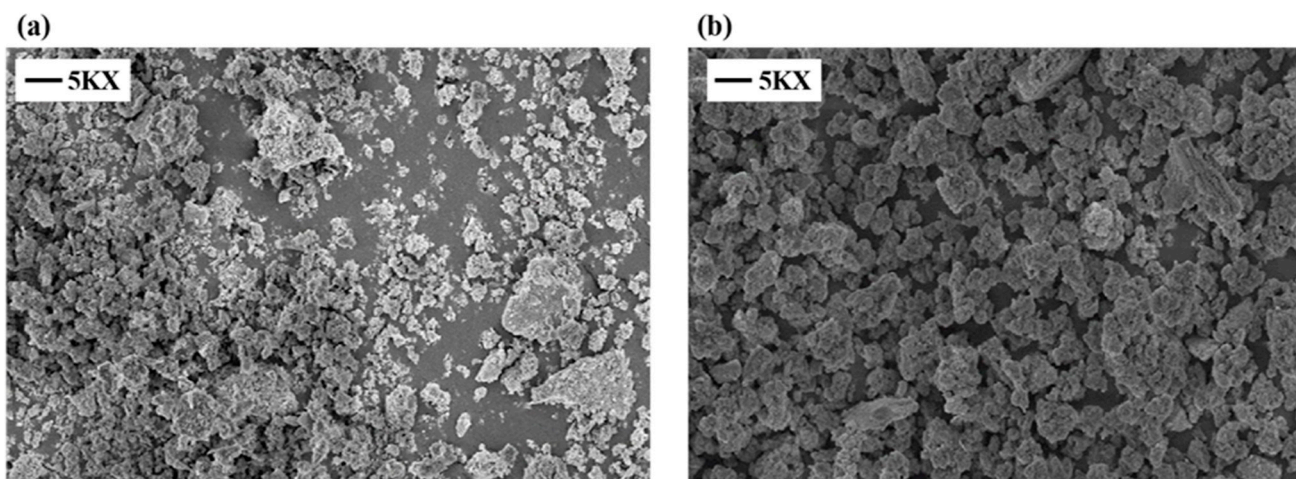


Figure 3. Surface morphological analysis of (a) RM (b) Ni/RM.

2.4.3. Elemental Analysis of Catalyst by Energy Dispersive X-Ray Analysis

The EDX analysis confirmed the elemental composition of the catalysts. From Figure 4, it can be seen that the RM support had a significant amount of Fe (around 60 wt%) and Al (around 15 wt%). The minor fractions include the presence of Si, Na, Ca, and Ti elements [23]. Further, the EDX analysis of metal-impregnated RM catalysts revealed the presence of Ni with a decrease in Fe (~45 wt%) and Na (~7–10 wt%) and a similar amount of the other elements of the freshly calcined RM support material [13]. This clearly states

that the actual composition of the red-mud catalyst was maintained without any significant loss of the elements.

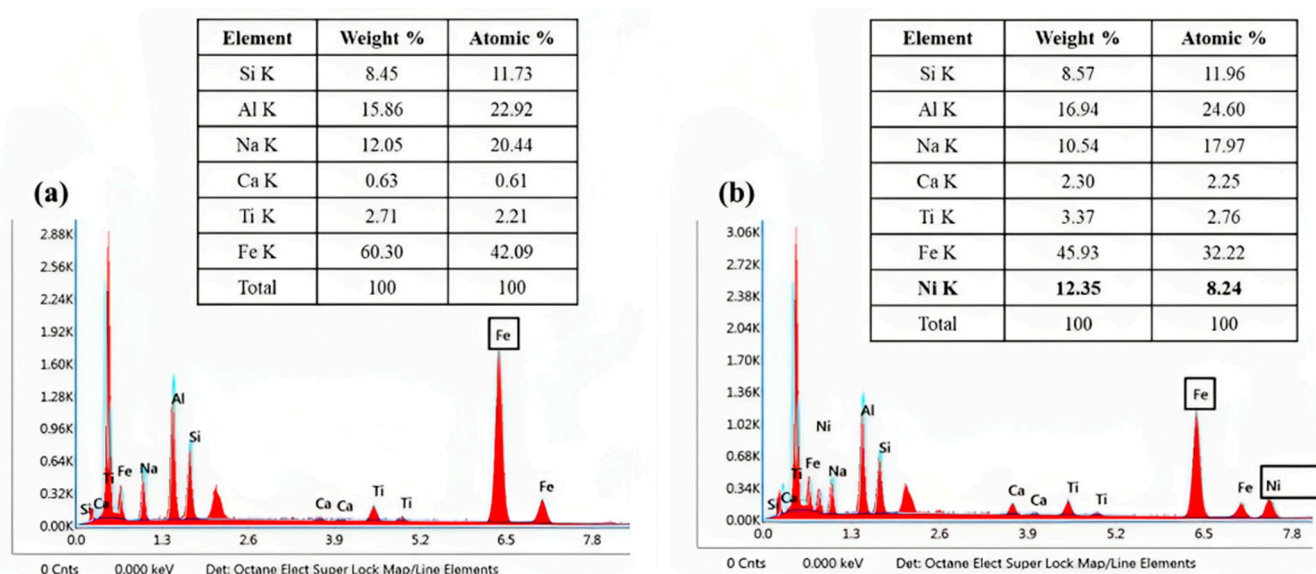


Figure 4. Elemental analysis of (a) RM (b) Ni/RM.

2.4.4. X-ray Diffraction Pattern of the Synthesized Catalysts

The XRD patterns of all the RM catalysts are also shown in Figure 5. In RM, the intensity of hematite and gibbsite peaks was higher than in metal-impregnated RM catalysts. Further, two crystalline peaks of NiO were detected at 2θ of 35° and 41° with related miller indices of (1 1 1) and (2 0 0), respectively. However, a peak of Ni was identified at 2θ of 62.5° (2 2 0). Therefore, the crystalline peaks of the Ni phase in RM catalysts signified their presence [13]. XRD peaks of RM catalysts also confirmed their composition. After observing the intensity of peaks, it can be stated that catalysts were also not highly crystalline.

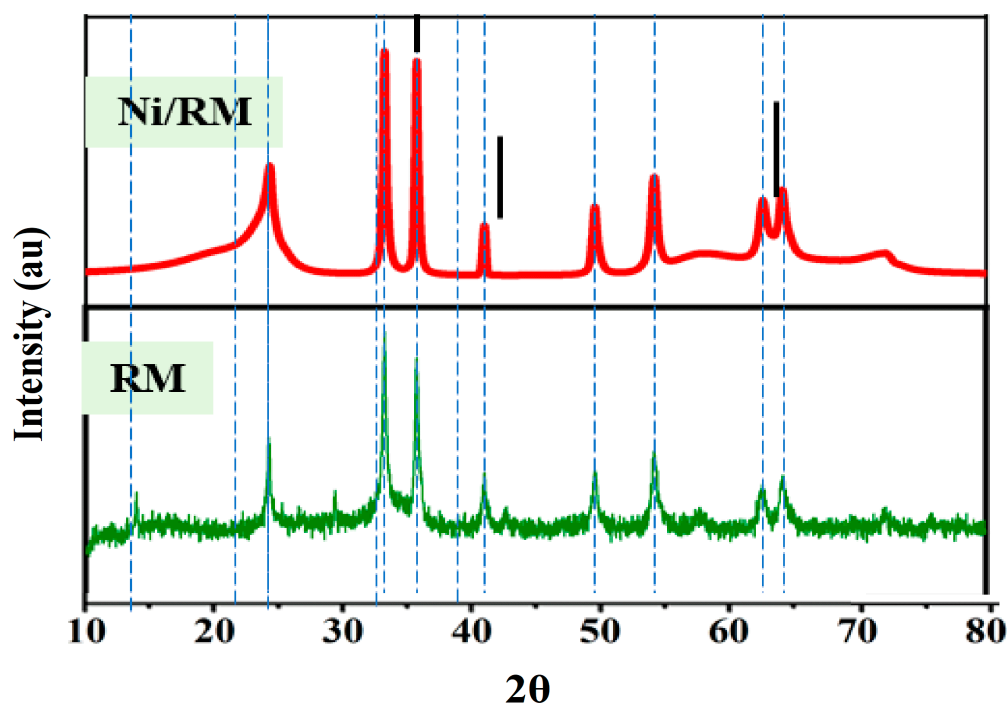


Figure 5. XRD analysis of RM and Ni/RM.

2.5. Thermal Pyrolysis and Pyrolytic Product Distribution

Thermal pyrolysis of MDC and GH feedstocks was conducted in batch mode in a fixed bed reactor at three different temperatures, namely 500, 550, and 600 °C. The yield of all the different pyrolytic products is presented in Figure 6. The thermal pyrolysis of *Mesua ferrea* de-oiled cake at 550 °C yielded a bio-oil of 11.34 wt% with a highest yield of 56.81 wt% of biochar and 31.85 wt% of non-condensable gases. In comparison, the thermal pyrolysis of garlic husk produced a maximum bio-oil yield of 12.31 wt% with biochar and non-condensable gases of 55.5 wt% and 32.19 wt%, respectively. The biochar yield is primarily high due to the high ash and lignin content of the feedstocks. During the pyrolysis process, the breakdown of cellulose and lignin led to an increase in the generation of bio-char and non-condensable gas products [24]. Alkali and alkaline earth metals in biomass stimulated secondary cracking processes converting condensable vapor into non-condensable gaseous products. The bio-oil production was lower for the thermal pyrolysis of both feedstocks.

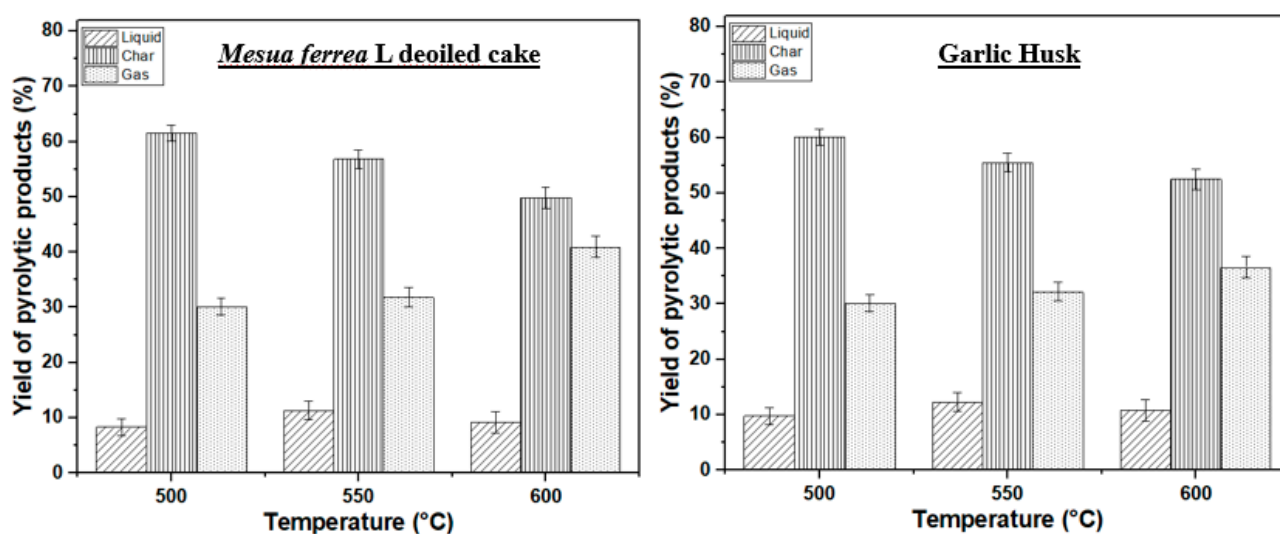


Figure 6. Thermal Pyrolysis of *Mesua ferrea* L. de-oiled cake and garlic husk.

Gas chromatography and mass spectroscopy (GC/MS) was used to analyze the different classes of organic compounds in the bio-oil. However, it is essential to note that the make-up of these chemicals changes significantly depending on the types of biomass used, the mode of pyrolysis, and the operating parameters of the process, among other factors. Hemicellulose and cellulose were pyrolyzed, and the principal products were aromatic hydrocarbons, acids, ketonic compounds, cycloalkane, furanic compounds, and other hydrocarbons [25]. The major compounds of the bio-oil obtained from the thermal pyrolysis of the MDC are Oleic acid (17.89%), Oleyl alcohol, chlorodifluoroacetate (12.41%), and Bis(2-ethylhexyl) phthalate (11.82%), followed by *cis*-9-Hexadecenal (6.64%) and 9-Octadecenoic acid (8.67%). Additionally, the GC-MS analysis of bio-oil derived from GH shows a strong presence of esters and phenols. Bis(2-ethylhexyl) phthalate (29.44%), 1,4,3,6-Dianhydro- α -D-glucopyranose (5.38%), Fenobucard (2.04%), Phenol, 3-ethyl (2.01%), Phenol, 2-methoxy (1.88%), and Phenol, 2,6-dimethoxy (1.64%), are the major compounds. In addition, the presence of alkanes shows the partial conversion of unsaturated fatty acids to alkanes [22]. The findings demonstrated that thermal pyrolytic oil could be used as a fuel for furnaces that provide residential heaters or as a solvent for extracting various valuable compounds. However, more advanced upgrading procedures, such as catalytic cracking, are required as a substitute for diesel fuel.

2.6. Catalytic Co-Pyrolysis and Pyrolytic Product Distribution

The primary characteristic of in situ catalytic pyrolysis is the direct blending of the catalyst with the raw materials, which are then introduced into the reactor for heating

and pyrolysis. This method ensures that the pyrolysis fragments come into contact with the catalyst for the first time, leading to enhanced pyrolysis and a reduced likelihood of secondary reactions of the pyrolysis products [26]. In comparison to oil obtained through conventional pyrolysis, catalytic co-pyrolytic oil demonstrates a substantial improvement in yield, increasing from 17.42 wt% to 20.31 wt% for RM catalyst, and 25.26 wt% for Ni/RM. It also exhibits a higher calorific value of 34.6 MJ kg⁻¹ for the Ni/RM catalyst.

Crude bio-oil is rich in intricate oxygenated compounds and almost exclusively composed of oxygenated organic substances, including unsaturated fatty acids, phenols, esters, and more. The oil derived from direct pyrolysis primarily comprises long carbon chain compounds with diverse end groups, whereas the catalytic bio-oil is predominantly composed of esters. During the upgrading process, the primary reactions involved the production of esters through the interaction of ketones, aldehydes, and carboxylic acids with ethanol, as validated by FTIR analysis. Additionally, rapid hydration reactions, esterification, and Friedel craft's acylation reaction took occurred, leading to the conversion of acid compounds into alkylated phenols and ester ethers. As a result of these transformations, the resulting product became less hydrophilic [3].

The bio-oil obtained from co-pyrolysis of MDC and GH contained a variety of compounds, such as phenol (1.86%), phenol-2-methyl (1.23%), p-cresol (3.11), 6-Octadecenoic acid (24.63%), n-hexadecanoic acid (5.52%), Indole (1.17%), and Octadecanoic acid (5.52%). These phenolic compounds might arise from the decomposition of lignin components, accounting for approximately 11% of the total area, whereas the fatty acid content was found to be 41.05%, as shown in Figure 7. The catalytic co-pyrolysis of the biomass was performed in the presence of red-mud and the Ni/RM catalyst. Based on the quantities yield of the bio-oil, the bio-oil produced from Ni/RM was further analysed for GC/MS to obtain the product composition. The primary fatty acids, such as n-hexadecanoic acid (15.17%), octadecanoic acid (6.57%), Bis(2-ethylhexyl) phthalate (4.25%), and oleic acid (1.36%), have increased while the amount 6-octadecanoic acid (12.52%) decreased when compared to co-pyrolysis, which accounts for a total of 38%. It is estimated that the fatty acids in bio-oil were originated from MDC feedstocks due to the oil content of the sample [5]. In addition, the phenolic content of the bio-oil was significantly reduced to 0.57% with p-cresol to be 0.29%. Additionally, a compound, namely Oleyl chloride, is present in significant quantity, which reacts with phenol to form esters [27]. This reaction is known as Friedel crafts acylation reaction, which requires Lewis acid sites facilitated by the Ni/RM catalyst. In addition, the conversion of Jasmonic acid (a primary plant inhibitor present in ripened fruit) to Propyl dihydroxy jasmoate (5%) is a major reaction that was observed in the catalytic co-pyrolytic oil [28].

Upon subjecting bio-oils to an ethanol/methanol solvent, a significant increase was observed in the concentration of various identified ester compounds and their corresponding area percentages. Conversely, the remaining esters could originate from the reaction between alcohols and acids, resulting from intermediate products derived from the conversion of oxygenated compounds [29]. When compared to acids, esters show greater potential for fuel composition as they have a reduced corrosive impact on the engine surface. It is possible that esters are formed through an esterification reaction involving the acids present in the bio-oil and alcohol. Methanol solvent used for the extraction of bio-oil generally aids in the reduction of long-chain fatty acids to convert them to esters [30].

Thus, a decline in oxygenated compounds and acid content, coupled with an increase in esters, indicates a highly effective catalyst activity, resulting in reduced viscosity and enhanced hydrophobicity of the final product [31]. Consequently, these alterations not only improve the stability of the upgraded bio-oil but also enhance its potential for hydrocarbon blending. Despite these changes, certain oxygenated compounds, such as aldehydes, phenols, and ketones, are still present in the upgraded bio-oil. These compounds possess persistent reactivity, primarily due to the presence of the carbonyl group, as evidenced by FTIR analysis peaks in the wavenumber range of 700–500 cm⁻¹. Compounds containing C = O bonds contribute to the reduced stability of the bio-oil [32].

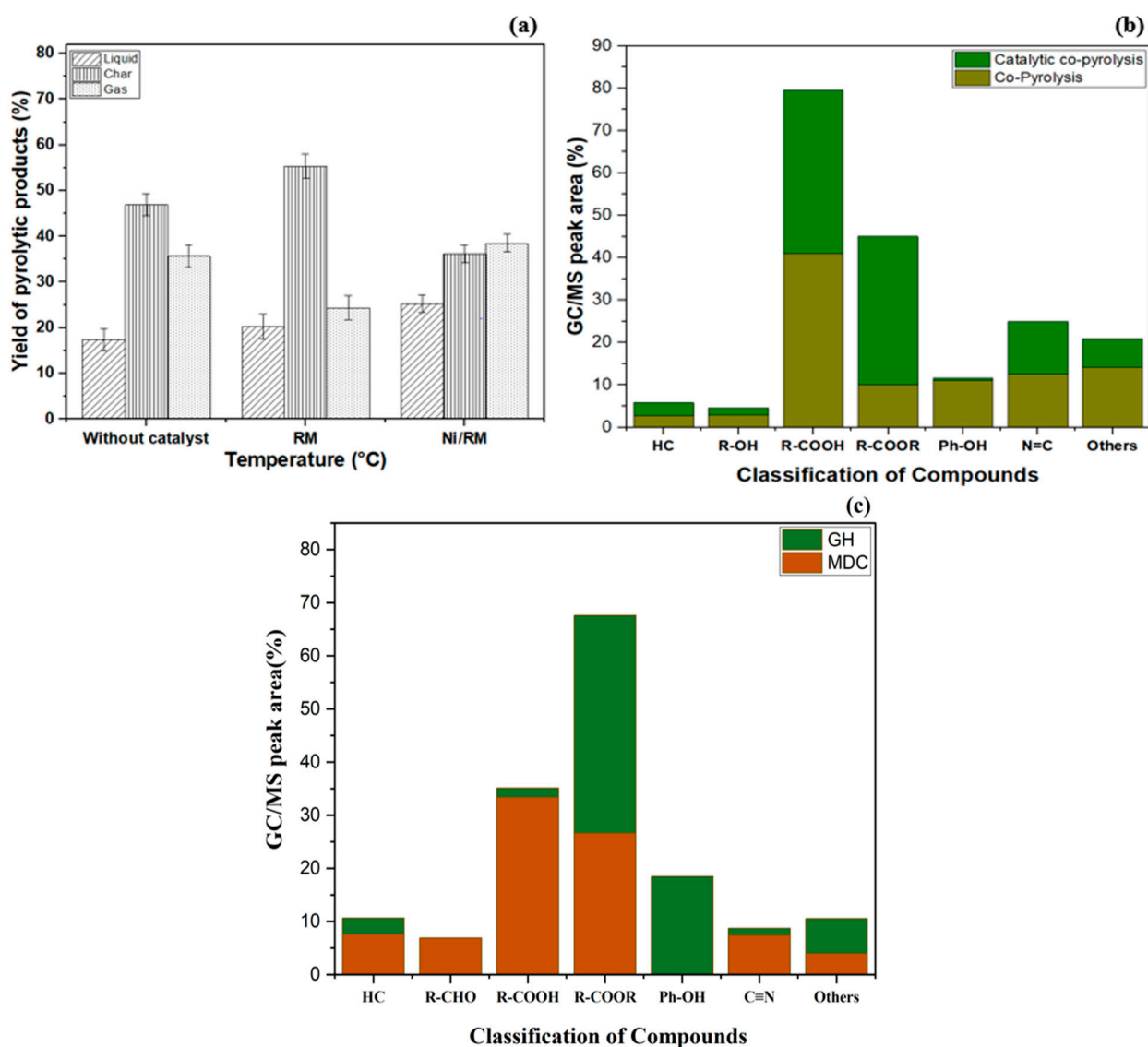


Figure 7. Catalytic co-pyrolysis: (a) Yield of Pyrolytic Products; (b) Pyrolytic product distribution of co-pyrolysis and catalytic co-pyrolysis by GC/MS analysis; (c) Pyrolytic product distribution of MDC and GH by GC/MS analysis.

3. Material and Methods

3.1. Materials

The biomass, namely de-oiled cake of *Mesua ferrea* L. oilseed and garlic husk, was collected from Assam, India. The biomass feedstocks were ground and passed through a mesh to obtain an average particle size of 1 mm. The detailed procedure for proximate and ultimate analysis of the ground biomasses is reported elsewhere [5].

The second waste source used in the current study is red mud supplied by the National Aluminum Company (NALCO), Damonjodi, Odisha, India. The wet red mud was allowed to oven dry prior to pulverization and then sieved to the required particle size. Before conducting the pyrolysis, the crushed particles were calcined at 550 °C in a muffle furnace (Make: Thermo Fisher Scientific, Waltham, MA, USA and model: BF51732PFMC-1) for 4 h.

Catalyst Preparation

The catalysts were synthesized using wet-impregnation method. A magnetic stirrer was used to mix 5 g of calcined RM with 100 mL of distilled water at room temperature for 10 h to obtain a slurry-like mixture. Ni/RM was prepared by dissolving 10 wt% of nickel

at ambient temperature. After that, the temperature was raised to 85 °C so that the water could be evaporated from the mixture to form a slurry-like paste. Subsequently, calcination at 550 °C for 4 h in a muffle furnace and drying in a hot air oven at 100 °C for 12 h to obtain the as-synthesized catalysts were performed.

3.2. Thermal, Co-Pyrolysis and Catalytic Co-Pyrolysis of Biomass

The pyrolysis of individual biomass samples and co-feed (1:1) and catalytic co-feed (B:C- 5:1 *w/w*) was conducted in a semi-batch operation in a fixed-bed reactor. The reactor body was made up of Inconel 800 with specifications as 7.3 cm OD × 43 cm L. The reactor was placed in an electric furnace capable of uniform heat provision throughout the surface of the reactor. Additionally, the furnace has a PID controller to vary parameters such as temperature, heating rate, and residence time. The nitrogen gas generally acts as a fluidizing/carrier gas and was allowed to pass through the bottom of the reactor at a flow rate of 150–200 mL min⁻¹, as shown in Figure 8. The hot vapors produced during the pyrolysis process were condensed using an allihn condenser through which a coolant of 10 °C is circulated. Moreover, all the vapor-phase transfer lines were well-insulated to avoid condensation, reducing the liquid product yield.

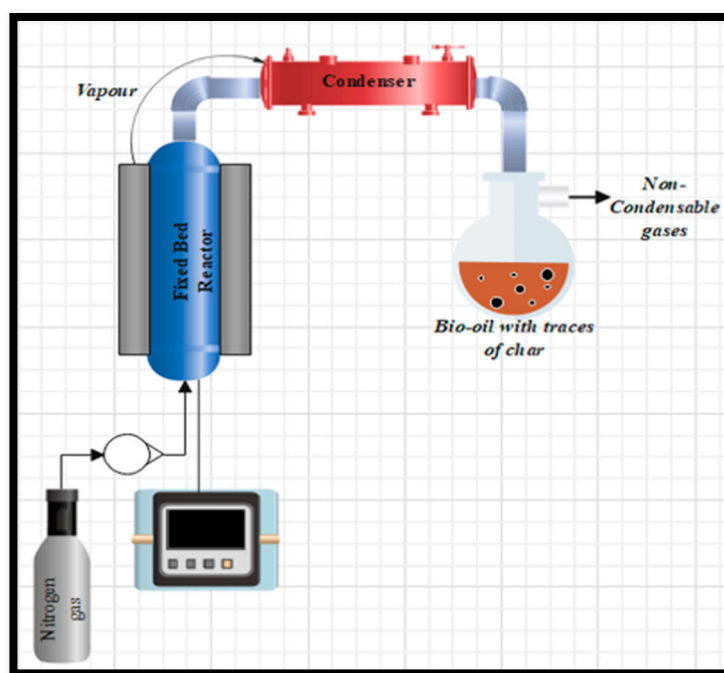


Figure 8. Schematic representation of fixed-bed pyrolysis reactor.

In the current study, the effect of temperature on the thermal pyrolysis of both biomass samples was investigated at 500–600 °C with a step of 50 °C and nitrogen flow rate of 150 mL min⁻¹ and at a heating rate of 10 °C min⁻¹. The optimal temperature found from the thermal pyrolysis was used to determine the yield of different products for the co-pyrolysis (1:1) and catalytic (RM, Ni/RM) co-pyrolysis ((B1/B2):C = 5:1) process. The yield of liquid product was calculated by noting the weight of the condensed vapor collected at the end of the experiments.

3.3. Biomass, Catalyst, and Pyrolytic Liquid Characterization

The thermal decomposition behaviour of biomass feedstocks and catalysts were performed using a thermo gravimetric analyser (Model No.: TG 209 F1 Libra; Make: M/s Netzsch, Selb, Germany). The samples were heated in a temperature range of 30–900 °C with a heating rate of 10 °C min⁻¹. Further, the functional group analysis of the biomass and the catalysts were obtained using FTIR spectroscopy in a wave number range of 400–4000 cm⁻¹.

Additionally, the energy potential (Higher Heating Value) of the biomass samples were determined using bomb calorimeter (Parr, Model: 1341 Plain Jacket Calorimeter).

The catalysts were characterized to study the crystalline nature, composition, and morphology. In order to conduct an X-ray diffraction (XRD) examination, a Make: Rigaku Technologies, Japan, Model: SmartLab diffractometer was employed, and it was set to 45 kV and 112 mA. The Cu K radiation used had a wavelength of 0.154 nm. With a step size of 0.2° , the analysis was conducted over a 2θ range of 10° to 80° . The morphology and composition of the different elements present in all three catalysts were investigated using FESEM and EDX using a Zeiss Sigma electron microscope. Brunauer-Emmett-Teller (BET) and Barrett-Joyner-Halenda (BJH) methods were used to measure the catalyst's surface area, pore size, and volume (TriStar II equipment, Micrometrics, Norcross, GA, USA).

The bio-oil sample obtained at optimized conditions, such as temperature and best-suited catalyst (based on the liquid yield percentage), was characterized using different techniques to find the structure of the compounds, as well as the energy potential of the samples. The pyrolytic liquid obtained from different pyrolysis conditions was extracted using two different solvents, namely methanol and cyclohexane, in the ratio of 1:2 *w/w* (Pyrolytic Liquid: Solvent). These extracted oils were separated from the solvents, and the solvent recovery was conducted using rota evaporation setup with a coolant (10°C) circulation. The higher heating value (HHV) of bio-oil was measured using a bomb calorimeter to determine the energy potential of the bio-oil obtained from different pyrolysis conditions.

The classification of compounds present in the sample was determined using GC-MS analysis. A gas chromatography having provision of an FID detector and an Elite-5MS column with specifications such as $60\text{ m} \times 0.25\text{ m} \times 0.25\ \mu\text{m}$ was used in the current study (Make: PerkinElmer and Model: Clarus 680 GC/600C MS). The stationary and mobile phases were chosen to be Dimethylpolysiloxane and diphenyl in a ratio of 0.95:0.05 (*v/v*). The flow rate of the phases was kept at 1 mL min^{-1} . A 0.002-mL sample was injected through the injection port, set at 280°C . The column conditions were set as follows: Initially, a program of 60°C for 1 min was set, and then the temperature was increased to 200°C at a heating rate of 7°C min^{-1} . Once the second step was reached, the temperature of the column was finally set to 300°C with a ramp rate of $10^\circ\text{C min}^{-1}$ with a holding time of 5 min. Mass spectrum analysis between 50 and 600 *m/z* was performed using an EI(+ve) mode operating at 70 eV. The structural details of the compounds were demonstrated using the NIST library.

4. Conclusions

In this study, the feasibility of *Mesua ferrea* L. de-oiled cake and garlic husk biomass as feedstock and co-feed for pyrolysis is studied. Additionally, the upgrading of bio-oil was tested using catalytic co-pyrolysis process. The effect of the temperature was observed on the thermal pyrolysis of both the individual feedstocks. As a result, 550°C was found to be the optimal temperature. This optimal temperature was then used for co-pyrolysis and catalytic co-pyrolysis of the feedstock. It was found that the addition of Ni/RM catalyst increased the bio-oil yield from 17.42 wt% to 25.46 wt%. Moreover, the addition of the catalyst led to the enhancement of the HHV by increasing the ester content of bio-oil. The main reaction pathways followed were: Friedel craft's acylation, Octadecanoid pathway reaction for the conversion of Jasmonic acid to Prohydrojasmon, and fatty acid conversion to alkanes and alkenes.

Author Contributions: Conceptualization, A.K. and K.M.; Formal analysis, A.K., J.K. and V.C.; Funding acquisition, K.M.; Investigation, A.K., J.K. and V.C.; Methodology, A.K., J.K. and V.C.; Supervision, K.M.; Validation, A.K.; Writing—original draft, A.K.; Writing—review & editing, K.M. All authors have read and agreed to the published version of the manuscript.

Funding: The authors would like to thank the Department of Science and Technology-Waste Management Technologies, India (S.O. DST/TDT/WMT/Plastic Waste/2021/09) and Hindustan Petroleum Corporation Ltd. (HPCL) R&D, Bangalore, India for funding the present research.

Data Availability Statement: Data will be available on request.

Acknowledgments: The authors would like to thank the Center for Environment, IIT Guwahati for the FTIR facility and the Central Instrument Facility (CIF), Analytical lab, Department of chemical Engineering, for the FESEM-EDX, XRD, BET, TGA facility in IIT Guwahati. Additionally, the Guwahati Biotech park located at Guwahati, Assam is acknowledged for providing the GC/MS and CHNS analytical facility.

Conflicts of Interest: The authors declare no conflict of interest.

References

1. Patel, P.K.; Pandey, L.M.; Uppaluri, R.V. Adsorptive removal of Zn, Fe, and Pb from Zn dominant simulated industrial wastewater solution using polyvinyl alcohol grafted chitosan variant resins. *Chem. Eng. J.* **2023**, *459*, 141563. [[CrossRef](#)]
2. Dorado, C.; Mullen, C.A.; Boateng, A.A. Origin of carbon in aromatic and olefin products derived from HZSM-5 catalyzed co-pyrolysis of cellulose and plastics via isotopic labeling. *Appl. Catal. B Environ.* **2015**, *162*, 338–345. [[CrossRef](#)]
3. Reshad, A.S.; Tiwari, P.; Goud, V.V. Thermal and co-pyrolysis of rubber seed cake with waste polystyrene for bio-oil production. *J. Anal. Appl. Pyrolysis* **2019**, *139*, 333–343. [[CrossRef](#)]
4. Komandur, J.; Mohanty, K. Chapter 2—Fast pyrolysis of biomass and hydrodeoxygenation of bio-oil for the sustainable production of hydrocarbon biofuels. In *Hydrocarbon Biorefinery*; Maity, S.K., Gayen, K., Bhowmick, T.K., Eds.; Elsevier: Amsterdam, The Netherlands, 2022; pp. 47–76. [[CrossRef](#)]
5. Komandur, J.; Vinu, R.; Mohanty, K. Pyrolysis kinetics and pyrolysate composition analysis of *Mesua ferrea* L.: A non-edible oilseed towards the production of sustainable renewable fuel. *Bioresour. Technol.* **2022**, *351*, 126987. [[CrossRef](#)] [[PubMed](#)]
6. Agrawalla, A.; Kumar, S.; Singh, R. Pyrolysis of groundnut de-oiled cake and characterization of the liquid product. *Bioresour. Technol.* **2011**, *102*, 10711–10716. [[CrossRef](#)] [[PubMed](#)]
7. Naresh Kumar, A.; Chatterjee, S.; Hemalatha, M.; Althuri, A.; Min, B.; Kim, S.-H.; Mohan, S.V. Deoiled algal biomass derived renewable sugars for bioethanol and biopolymer production in biorefinery framework. *Bioresour. Technol.* **2020**, *296*, 122315. [[CrossRef](#)]
8. Singh, R.K.; Patil, T.; Sawarkar, A.N. Pyrolysis of garlic husk biomass: Physico-chemical characterization, thermodynamic and kinetic analyses. *Bioresour. Technol. Rep.* **2020**, *12*, 100558. [[CrossRef](#)]
9. Zhang, W.; Yuan, C.; Xu, J.; Yang, X. Beneficial synergetic effect on gas production during co-pyrolysis of sewage sludge and biomass in a vacuum reactor. *Bioresour. Technol.* **2015**, *183*, 255–258. [[CrossRef](#)]
10. Zuo, W.; Jin, B.; Huang, Y.; Sun, Y. Characterization of top phase oil obtained from co-pyrolysis of sewage sludge and poplar sawdust. *Environ. Sci. Pollut. Res.* **2014**, *21*, 9717–9726. [[CrossRef](#)]
11. Chen, D.; Cen, K.; Chen, F.; Zhang, Y. Solar pyrolysis of cotton stalks: Combined effects of torrefaction pretreatment and HZSM-5 zeolite on the bio-fuels upgradation. *Energy Convers. Manag.* **2022**, *261*, 115640. [[CrossRef](#)]
12. Valizadeh, S.; Ko, C.H.; Lee, J.; Lee, S.H.; Yu, Y.J.; Show, P.L.; Rhee, G.H.; Park, Y.-K. Effect of eggshell- and homo-type Ni/Al₂O₃ catalysts on the pyrolysis of food waste under CO₂ atmosphere. *J. Environ. Manag.* **2021**, *294*, 112959. [[CrossRef](#)] [[PubMed](#)]
13. Jahromi, H.; Agblevor, F.A. Hydrodeoxygenation of pinyon-juniper catalytic pyrolysis oil using red mud-supported nickel catalysts. *Appl. Catal. B Environ.* **2018**, *236*, 1–12. [[CrossRef](#)]
14. Qiu, Z.; Zhai, Y.; Li, S.; Liu, X.; Liu, X.; Wang, B.; Liu, Y.; Li, C.; Hu, Y. Catalytic co-pyrolysis of sewage sludge and rice husk over biochar catalyst: Bio-oil upgrading and catalytic mechanism. *Waste Manag.* **2020**, *114*, 225–233. [[CrossRef](#)] [[PubMed](#)]
15. Kaur, R.; Kumar, V.T.; Krishna, B.B.; Bhaskar, T. Characterization of slow pyrolysis products from three different cashew wastes. *Bioresour. Technol.* **2023**, *376*, 128859. [[CrossRef](#)] [[PubMed](#)]
16. Komandur, J.; Kumar, A.; Para, P.; Mohanty, K. Kinetic Parameters Estimation of Thermal and Co-Pyrolysis of Groundnut De-oiled Cake and Polyethylene Terephthalate (PET) Waste. *Energies* **2022**, *15*, 7502. [[CrossRef](#)]
17. Setter, C.; Silva, F.T.M.; Assis, M.R.; Ataíde, C.H.; Trugilho, P.F.; Oliveira, T.J.P. Slow pyrolysis of coffee husk briquettes: Characterization of the solid and liquid fractions. *Fuel* **2020**, *261*, 116420. [[CrossRef](#)]
18. Sharma, R.; Sheth, P.N. Multi reaction apparent kinetic scheme for the pyrolysis of large size biomass particles using macro-TGA. *Energy* **2018**, *151*, 1007–1017. [[CrossRef](#)]
19. Abu Bakar, M.S.; Titiloye, J.O. Catalytic pyrolysis of rice husk for bio-oil production. *J. Anal. Appl. Pyrolysis* **2013**, *103*, 362–368. [[CrossRef](#)]
20. Wahyudi, A.; Kurniawan, W.; Hinode, H. Study on Deactivation and Regeneration of Modified Red Mud Catalyst Used in Biodiesel Production. *Green Sustain. Chem.* **2017**, *7*, 247–258. [[CrossRef](#)]
21. Rammohan, D.; Kishore, N.; Uppaluri, R.V.S. Reaction kinetics and thermodynamic analysis of non-isothermal co-pyrolysis of *Delonix regia* and tube waste. *Bioresour. Technol. Rep.* **2022**, *18*, 101032. [[CrossRef](#)]

22. Chen, J.; Wang, D.; Luo, F.; Yang, X.; Li, X.; Li, S.; Ye, Y.; Wang, D.; Zheng, Z. Selective production of alkanes and fatty alcohol via hydrodeoxygenation of palmitic acid over red mud-supported nickel catalysts. *Fuel* **2022**, *314*, 122780. [[CrossRef](#)]
23. Wang, Y.; Wang, Y.; Lu, X.; Sun, W.; Xu, Y.; Zhou, J. Catalytic Ozonation for Effective Degradation of Coal Chemical Biochemical Tail Water by Mn/Ce@RM Catalyst. *Water* **2022**, *14*, 206. [[CrossRef](#)]
24. Shadangi, K.P.; Singh, R.K. Thermolysis of polanga seed cake to bio-oil using semi batch reactor. *Fuel* **2012**, *97*, 450–456. [[CrossRef](#)]
25. Wang, Y.; Akbarzadeh, A.; Chong, L.; Du, J.; Tahir, N.; Awasthi, M.K. Catalytic pyrolysis of lignocellulosic biomass for bio-oil production: A review. *Chemosphere* **2022**, *297*, 134181. [[CrossRef](#)] [[PubMed](#)]
26. Baloch, H.A.; Siddiqui, M.T.H.; Nizamuddin, S.; Mubarak, N.M.; Khalid, M.; Srinivasan, M.P.; Griffin, G.J. Solvothermal co-liquefaction of sugarcane bagasse and polyethylene under sub-supercritical conditions: Optimization of process parameters. *Process. Saf. Environ. Prot.* **2020**, *137*, 300–311. [[CrossRef](#)]
27. Heravi, M.M.; Zadsirjan, V.; Saedi, P.; Momeni, T. Applications of Friedel–Crafts reactions in total synthesis of natural products. *RSC Adv.* **2018**, *8*, 40061–40163. [[CrossRef](#)]
28. Blechert, S.; Brodschelm, W.; Hölder, S.; Kammerer, L.; Kutchan, T.M.; Mueller, M.J.; Xia, Z.Q.; Zenk, M.H. The octadecanoic pathway: Signal molecules for the regulation of secondary pathways. *Proc. Natl. Acad. Sci. USA* **1995**, *92*, 4099–4105. [[CrossRef](#)]
29. Omar, S.; Alsamaq, S.; Yang, Y.; Wang, J. Production of renewable fuels by blending bio-oil with alcohols and upgrading under supercritical conditions. *Front. Chem. Sci. Eng.* **2019**, *13*, 702–717. [[CrossRef](#)]
30. Zhang, J.; Luo, Z.; Dang, Q.; Wang, J.; Chen, W. Upgrading of Bio-oil over Bifunctional Catalysts in Supercritical Monoalcohols. *Energy Fuels* **2012**, *26*, 2990–2995. [[CrossRef](#)]
31. Baloch, H.A.; Nizamuddin, S.; Siddiqui, M.T.H.; Riaz, S.; Konstas, K.; Mubarak, N.M.; Srinivasan, M.P.; Griffin, G.J. Catalytic upgradation of bio-oil over metal supported activated carbon catalysts in sub-supercritical ethanol. *J. Environ. Chem. Eng.* **2021**, *9*, 105059. [[CrossRef](#)]
32. Ichihashi, Y.; Kamizaki, Y.-H.; Terai, N.; Taniya, K.; Tsuruya, S.; Nishiyama, S. One-Step Oxidation of Benzene to Phenol over Cu/Ti/HZSM-5 Catalysts. *Catal. Lett.* **2010**, *134*, 324–329. [[CrossRef](#)]

Disclaimer/Publisher’s Note: The statements, opinions and data contained in all publications are solely those of the individual author(s) and contributor(s) and not of MDPI and/or the editor(s). MDPI and/or the editor(s) disclaim responsibility for any injury to people or property resulting from any ideas, methods, instructions or products referred to in the content.